

Synthesis, Characterization, and Pharmacokinetic Evaluation of a Potential MRI Contrast Agent Containing Two Paramagnetic Centers with Albumin Binding Affinity

Tatjana N. Parac-Vogt,^[a] Kristof Kimpe,^[a] Sophie Laurent,^[b] Luce Vander Elst,^[b] Carmen Burtea,^[b] Feng Chen,^[c] Robert N. Muller,^[b] Yicheng Ni,^[c] Alfons Verbruggen,^[d] and Koen Binnemans^{*,[a]}

Abstract: A dinuclear gadolinium(III) complex of an amphiphilic chelating ligand, containing two diethylenetriamine-*N,N,N',N'',N'''*-pentaacetate (DTPA) moieties bridged by a bisindole derivative with three methoxy groups, has been synthesized and evaluated as a potential magnetic resonance imaging (MRI) contrast agent. Nuclear magnetic relaxation dispersion (NMRD) measurements indicate that at 20 MHz and 37 °C the dinuclear gadolinium(III) complex has a much higher relaxivity than [Gd(DTPA)] (6.8 vs 3.9 s⁻¹ mmol⁻¹). The higher relaxivity of the dinuclear gadolinium(III) complex can be related to its reduced motion and larger rotational correlation time relative to [Gd(DTPA)]. In

the presence of human serum albumin (HSA) the relaxivity value of the non-covalently bound dinuclear complex increases to 15.2 s⁻¹ per mmol of Gd³⁺, due to its relatively strong interaction with this protein. The fitted value of the binding constant to HSA (K_a) was found to be 10⁴ M⁻¹. Because of its interaction with HSA, the dinuclear complex exhibits a longer elimination half-life from the plasma, and a better confinement to the vascular space compared to the commercially available [Gd(DTPA)] contrast agent. Transme-

talation of the dinuclear gadolinium(III) complex by zinc(II) has been investigated. Biodistribution studies suggest that the complex is excreted by the renal pathway, and possibly by the hepatobiliary route. In vivo studies indicated that half of the normal dose of the gadolinium(III) complex enhanced the contrast in hepatic tissues around 40% more effectively than [Gd(DTPA)]. The dinuclear gadolinium(III) complex was tested as a potential necrosis avid contrast agent (NACA), but despite the binding to HSA, it did not exhibit necrosis avidity, implying that binding to albumin is not a key parameter for necrosis-targeting properties.

Keywords: gadolinium • imaging agents • lanthanides • NMR spectroscopy • rare earths

Introduction

Magnetic resonance imaging (MRI) is routinely used in various diagnostic imaging procedures. Although excellent soft-tissue images can be obtained by this method, early experi-

ments showed that contrast agents might greatly increase its diagnostic value. Consequently, the development of MRI techniques has been accompanied by an increased interest in developing contrast agents.^[1-3] The first MRI contrast agent approved for use in humans, the gadolinium(III) com-


[a] Dr. T. N. Parac-Vogt, Dr. K. Kimpe, Prof. Dr. K. Binnemans
Department of Chemistry, Katholieke Universiteit Leuven
Celestijnenlaan 200F, 3001 Leuven (Belgium)
Fax: (+32) 16-327-992
E-mail: koen.binnemans@chem.kuleuven.ac.be

[b] Dr. S. Laurent, Prof. Dr. L. Vander Elst, Dr. C. Burtea,
Prof. Dr. R. N. Muller
NMR and Molecular Imaging Laboratory
Department of Organic and Biomedical Chemistry
University of Mons-Hainaut, 7000 Mons (Belgium)

[c] Dr. F. Chen, Prof. Dr. Y. Ni
Biomedical Imaging
Interventional Therapy and Contrast Media Research

Department of Radiology, University Hospitals, K.U. Leuven
Herestraat 49, 3000 Leuven (Belgium)

[d] Prof. Dr. A. Verbruggen
Laboratory of Radiopharmaceutical Chemistry
Department of Pharmaceutical Sciences
Van Evenstraat 4, 3000 Leuven (Belgium)

 Supporting information for this article is available on the WWW under <http://www.chemeurj.org/> or from the author.

plex of diethylenetriamine-*N,N,N',N',N''*-pentaacetate, [Gd(DTPA)], is used in clinical MRI under the name Magnevist®. This prototype of the first generation of contrast agents distributes into the vascular and interstitial space and is classified as an “unspecific agent” or “extracellular fluid agent”. In recent years, efforts have been directed towards the development of contrast agents that are tissue specific with higher proton relaxivities.

Higher proton relaxivity can be achieved by slowing the rotational motion of the contrast agent. Various routes have been explored to increase correlation time, such as the incorporation of the contrast agent into liposomes.^[4,5] Although incorporation of paramagnetic compounds into liposomes efficiently increases rotational correlation time, the application of these particles *in vivo* has some disadvantages, such as their rapid physiological removal by Kupffer cells of the liver and spleen, and their relatively slow clearance rate, which may be harmful to human tissue.^[6] An alternative strategy is the synthesis of macromolecular gadolinium(III) chelates, such as dendrimers,^[7] linear polymers,^[8–10] or proteins.^[2,11–12] This strategy, however, has proved to be rather disappointing, as the relaxivity gained by increasing the molecular size is often much less than expected, because of the internal flexibility or nonrigid attachment of the chelate to the macromolecule.^[7–14] More recently, an increase in rotational correlation time was achieved by either incorporating amphiphilic gadolinium(III) chelates into mixed micelles,^[15,16] or by designing complexes that can self-assemble to form micelles.^[17,18] Due to their reduced particle size (50 nm or less), these agents are less recognizable by the Kupffer cells for physiological removal, with the result that their residence time in blood increases. Consequently, they could be very promising as potential MRI contrast agents.^[15,19]

The so-called noncovalent binding strategy offers an alternative to the macromolecular approach,^[20,21] and involves targeting of a small gadolinium(III) complex to a particular protein. Binding to a protein increases the concentration of the complex around the protein receptor molecule, which selectively enhances the target relative to the background. The first example of this type of contrast agent was [MS-325], a compound designed to image the blood pool by exploiting its noncovalent binding to the plasma protein human serum albumin (HSA).^[22–24] This biophysical trick limits the amount of free drug that can extravasate from the blood pool into the nonvascular space, and provides selective enhancement of the vascular relaxation rate. In addition, this noncovalent binding causes a further slowing of the rotational motion, resulting in a much higher relaxivity.^[14,25] This binding mechanism has also been related to necrosis avidity (i.e., detection of necrotic tissue).^[26]

Recently, heteroditopic ligands featuring a DTPA- or DOTA-like unit for the chelation of gadolinium(III) (DOTA = 1,4,7,10-tetraazacyclododecane-1,4,7,10-tetraacetic acid), and a phenanthroline or terpyridine unit able to form highly stable complexes with iron(II), have been designed.^[27] The resulting spontaneous formation of high molecular

weight, supramolecular complexes increases the rotational correlation time, and the presence of multiple paramagnetic centers results in an increased relaxivity. Complexes containing multiple gadolinium(III) chelate units designed as blood-pool contrast agents have been reported by Martin et al.^[28] More recently, heterocyclic complexones containing two pyrazole rings and two iminodiacetic units per molecule have been shown to bind two gadolinium(III) ions.^[29] Although the observed relaxivity was improved significantly relative to [Gd(DTPA)] and [Gd(DOTA)], the thermodynamic stability of the complexes was low, probably because of only tetradentate coordination around the gadolinium(III) ion.

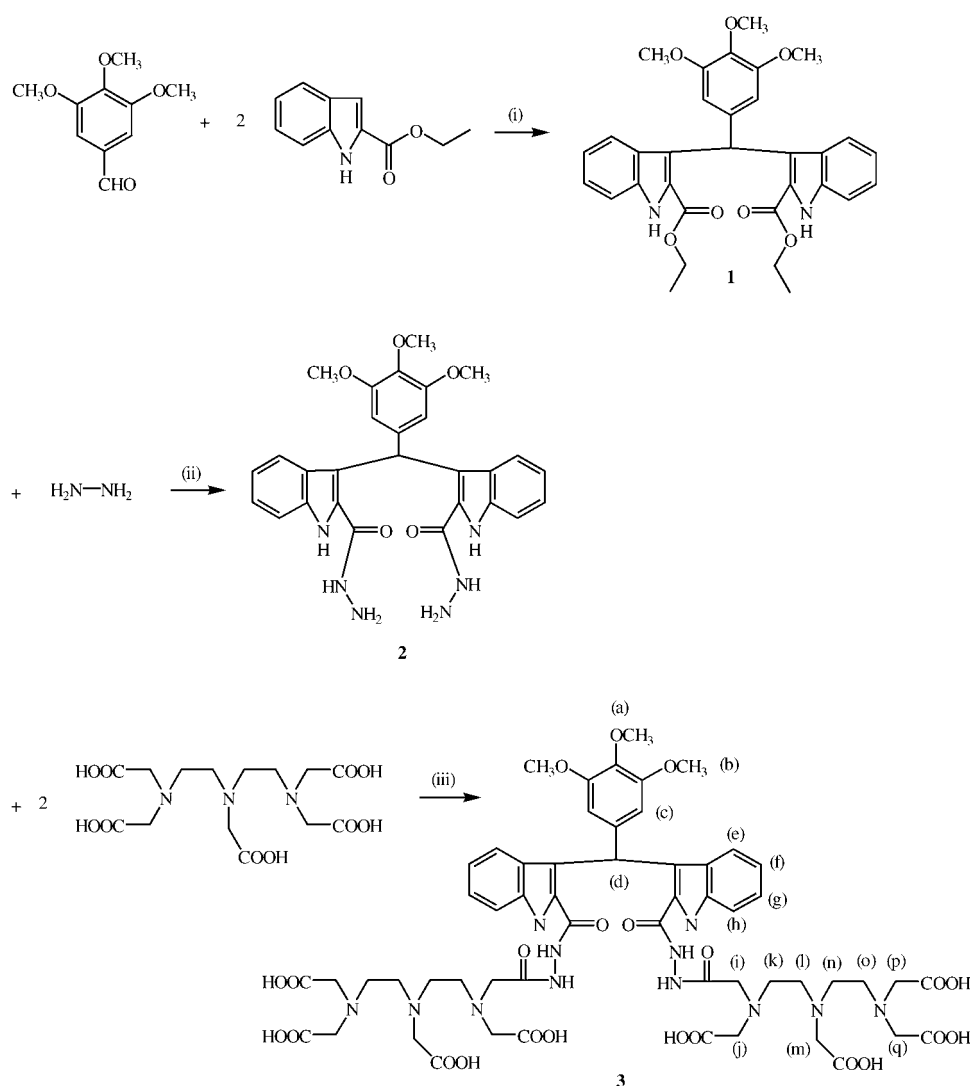
In the search for more efficient and specific contrast agents, we designed a novel amphiphilic ligand bearing two DTPA units capable of forming stable octacoordinate complexes with two gadolinium(III) ions. The two DTPA units are linked by a 2,3-disubstituted bisindole derivative, and we anticipated that this type of linker would noncovalently bind to plasma proteins. By using this approach, relaxivity was increased not only by the presence of multiple paramagnetic centers, but also by the reduced rate of molecular tumbling.

The dinuclear gadolinium(III) complex was characterized, preclinically evaluated, and tested *in vivo*. Its ability to bind to albumin was also examined, and because it has been suggested that the albumin binding mechanism may be the reason for necrosis avidity,^[26] the dinuclear gadolinium(III) complex was also tested for necrosis-targeting applications.

Results and Discussion

The ligand and complexes: The key difference between our design of ligand **3** (Scheme 1) and the approach used for other agents with high albumin affinity (such as [MS-325]),^[22–25] was the use of the lipophilic group, which can bind two DTPA moieties, as a starting point. A bisindole derivative of trimethoxybenzaldehyde, **1**, was chosen as the basis for the attachment of two DTPA moieties. Hydrazine was used as a bridging molecule because of its ability to form two amide bonds. The first amide bond is formed by reaction of hydrazine with the ethylcarboxylate group of the ethylindole-2-carboxylate moiety. Compound **2**, formed by this reaction, was further coupled in the presence of the coupling agent *o*-benzotriazol-1-yl-*N,N,N',N'*-tetramethyluronium tetrafluoroborate (TBTU) to two DTPA molecules to yield ligand **3**.

The ¹H NMR spectrum of this final product (Figure 1) was recorded in D₂O and its full assignment was achieved by conducting two-dimensional COSY experiments (see Supporting Information). The spectrum consists of 16 signals, which indicate the symmetry of the ligand molecule (see Scheme 1 for labeling). Electrospray mass spectrometry (ES-MS) was used to confirm the structure of ligand **3** in solution. The ES-MS spectrum in the positive mode showed a molecular peak [M+Na]⁺ at *m/z* 1301.4, consistent with the structure shown in Scheme 1.



Scheme 1. Synthesis of ligand **3**. Conditions: i) reflux in EtOH/conc. HCl; ii) MeOH/pyridine, 100 °C; iii) TBTU/TEA, DMSO.

Under slightly alkaline conditions, the ligand readily formed complexes with lanthanide(III) ions (Ln = La, Gd). IR spectral data of the ligand showed strong absorptions in

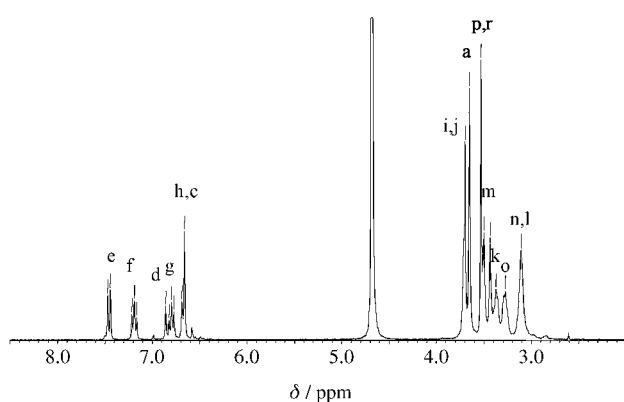


Figure 1. Proton NMR spectrum of ligand **3** in D₂O at 298 K. For the resonance assignment, see Scheme 1.

the region 1690–1625 cm⁻¹, corresponding to CO stretching modes. A shift of approximately 50 cm⁻¹ to lower energy was observed for the carbonyl stretching frequencies after complexation, indicating amide oxygen coordination to the lanthanide ion. Positive mode ES-MS of the lanthanum(III) and gadolinium(III) complexes showed molecular peaks at *m/z* 1595 and 1632, respectively, indicating the binding of two metal ions to the ligand. This finding was also supported by elemental analysis data. The solution structure of the dinuclear complex was investigated by recording the proton NMR spectrum of the lanthanum(III) complex. Complexation of **3** to lanthanum(III) causes remarkable changes in the proton NMR spectra in the form of shifts and broadening of the resonances. Although the proton resonances of the ligand are sharp and well separated, the resonances of the lanthanum(III) complex are very broad, and multiple peaks were observed for the protons adjacent to the carboxylic groups. Heating the solution to 368 K resulted in the severe broadening of all the resonances (see Supporting Information). The

spectra are consistent with the occurrence of several interconverting isomers; a typical characteristic of lanthanide(III) complexes with DTPA ligands.^[30] However, based on the available NMR spectroscopy data, no speculation on the structures of the isomers present in the solution is possible. Unfortunately, we were unable to grow crystals of sufficient quality to allow structure determination by X-ray single crystal diffraction; however, the IR, ES-MS, and elemental analysis data are consistent with the formation of a dinuclear complex in which two lanthanide(III) ions are coordinated to two DTPA moieties. From hereon, the dinuclear gadolinium(III) complex is denoted [Gd₂-**3**].

Residence time of the coordinated water molecule in [Gd₂-3**]:** The residence time of the coordinated water molecule (τ_M) was obtained by analysis of the temperature dependence of the reduced transverse relaxation rate of the water ¹⁷O nucleus in solutions of the gadolinium complex (Figure 2). The theoretical adjustment of these experimental

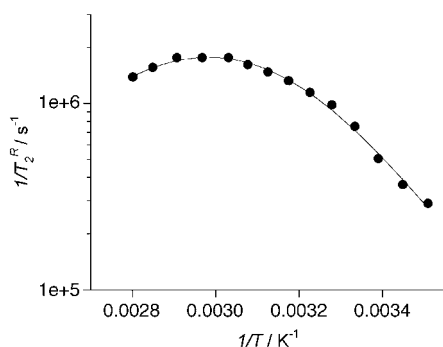


Figure 2. Evolution of the reduced ^{17}O transverse relaxation rate ($R_2^{\text{para}} \approx 55.55/\text{Gd}^{\text{III}}$ concentration) versus the reciprocal of the temperature for $[\text{Gd}_2\text{-3}]$. Concentration of $[\text{Gd}_2\text{-3}] = 12.42 \text{ mM}$.

data was performed as previously described, assuming the presence of one water molecule in the first coordination sphere.^[31] This procedure allows for the determination of:

1. The hyperfine coupling constant (A/\hbar) between the oxygen nucleus of bound water molecules and the gadolinium(III) ion.
2. Parameters describing the electronic relaxation times of Gd^{3+} , that is, the correlation time modulating the electronic relaxation (τ_v), the activation energy (E_v) related to τ_v , and the mean-square of the zero-field splitting energy Δ^2 .
3. Parameters related to the water exchange, that is, the enthalpy (ΔH^\ddagger) and entropy (ΔS^\ddagger) of activation of the process.

At 310 K, the water residence time of $[\text{Gd}_2\text{-3}]$ is equal to $599 \pm 32 \text{ ns}$ (Table 1). This value is greater than that for both the parent compound $[\text{Gd}(\text{DTPA})]$ ($\tau_M^{310} = 132 \text{ ns}$ ^[31b] and

Table 1. Parameters for $[\text{Gd}_2\text{-3}]$ obtained from the theoretical fitting of the ^{17}O NMR data. Parameters for $[\text{Gd}(\text{DTPA})]$ and $[\text{MS-325}]$ are shown for comparison.

Parameter	$[\text{Gd}_2\text{-3}]$	$[\text{Gd}(\text{DTPA})]$	$[\text{MS-325}]$
τ_M^{310} [ns]	599 ± 32	143 ± 25	83 ± 13 ^[a]
ΔH^\ddagger [kJ mol^{-1}]	49.4 ± 0.1	51.5 ± 0.3	51.3 ± 0.3 ^[a] 53.0 ± 1.8 ^[b]
ΔS^\ddagger [$\text{J mol}^{-1} \text{K}^{-1}$]	33.5 ± 0.2	52.1 ± 0.6	55.8 ± 0.4 ^[a]
A/\hbar [10^6 rad s^{-1}]	-4.0 ± 0.1	-3.4 ± 0.1	-4.1 ± 0.06 ^[a] -3.8 ^[b]
Δ^2 [10^{20} s^{-2}]	0.71 ± 0.06	1.08 ± 0.03	2.18 ± 0.10 ^[a] 0.25 ± 0.06 ^[b]
τ_v [298 K, ps]	10.0 ± 1.0	12.3 ± 0.3	18.7 ± 0.9 ^[a] 1.7 ± 0.1 ^[b]

[a] From ref. [25a]. [b] From ref. [25c].

143 ns ^[31a] and the albumin-binding $[\text{MS-325}]$ ($\tau_M^{310} = 83 \text{ ns}$),^[25b] but smaller than that reported for the DTPA-bisamide derivative $[\text{Gd}(\text{DTPA-BMA})]$ ($\tau_M^{310} = 1050 \text{ ns}$)^[31b] (DTPA-BMA = 1,7-bis[(*N*-methylcarbamoyl)methyl]-1,4,7-tris(carboxymethyl)-1,4,7-triazaheptane). The water residence time is in good agreement with the values reported

for other monoamide derivatives of $[\text{Gd}(\text{DTPA})]$, such as $[\text{Gd}(\text{DTPA-N-MA})]$ ($\tau_M^{310} = 346 \text{ ns}$),^[1b] and with the previously reported dimeric complexes based on DOTA ligands $[\text{Gd}(\text{pip}(\text{DO3A})_2)]$ ($\tau_M^{310} = 372 \text{ ns}$)^[31b] and $[\text{Gd}(\text{bisoxa}(\text{DO3A})_2)]$ ($\tau_M^{310} = 394 \text{ ns}$)^[31b] (DOTA = 1,4,7,10-tetrakis(carboxymethyl)-1,4,7,10-tetraazacyclododecane, DO3A = 1,4,7,10-tetraazacyclododecane-1,4,7-triacetic acid, $\text{pip}(\text{DO3A})_2 = \text{bis}(1,4\text{-}(1\text{-}(\text{carboxymethyl})\text{-}1,4,7,10\text{-tetraaza-}4,7,10\text{-tris}(\text{carboxymethyl})\text{-}1\text{-cyclododecyl-}1,4\text{-diazacyclohexane})\text{-}1,4,7,10\text{-tris}(\text{carboxymethyl})\text{-}1\text{-cyclododecyl})\text{-}1,10\text{-diaz-}3,6\text{-dioxadecane}$).

The scalar coupling constant (A/\hbar) is in good agreement with those values reported for other gadolinium(III) polyaminocarboxylate complexes that have one inner-sphere water molecule (typically $-3.8 \times 10^6 \text{ rad s}^{-1}$).^[31b] Inspection of the data listed in Table 1 reveals that, except for an entropy of activation (ΔS^\ddagger) somewhat lower than for $[\text{Gd}(\text{DTPA})]$ and $[\text{MS-325}]$, all other parameters determined for $[\text{Gd}_2\text{-3}]$ are within the normal range observed for gadolinium(III) chelates.

Nuclear magnetic relaxation dispersion (NMRD) measurements of $[\text{Gd}_2\text{-3}]$: The $[\text{Gd}_2\text{-3}]$ dinuclear complex was investigated by recording ^1H longitudinal relaxation time measurements in water at 310 K and at magnetic field strengths ranging from 0.24 mT to 1.4 T. The proton NMRD profile recorded at 310 K (Figure 3) shows that at high magnetic fields the proton relaxivity of $[\text{Gd}_2\text{-3}]$, expressed in $\text{s}^{-1} \text{ mmol}^{-1}$ of Gd^{3+} per liter, is much larger than that of the parent $[\text{Gd}(\text{DTPA})]$ compound. The data were analyzed by using the classical inner-sphere^[32,33] and outer-sphere^[34] theories. Some parameters were fixed during the fitting procedure: the distance (d) of closest approach for the outer-sphere contribution was set at 0.36 nm, the τ_M value was obtained by performing ^{17}O NMR spectroscopy as described above, and the number of water molecules in the first coordination sphere of Gd^{3+} was set to one, in agreement with

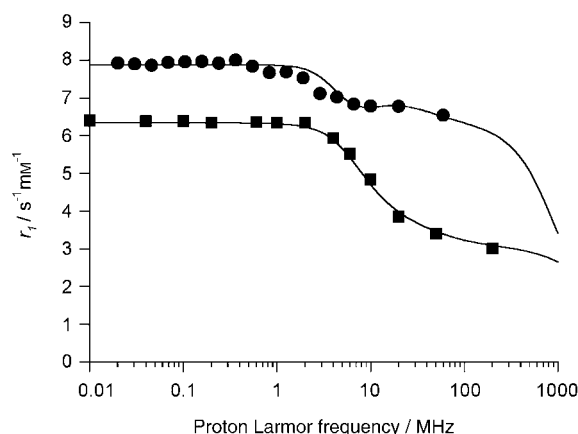


Figure 3. Proton NMRD profile of $[\text{Gd}_2\text{-3}]$ in water at 310 K (\bullet). The NMRD profile of $[\text{Gd}(\text{DTPA})]$ is added for comparison (\blacksquare).^[31] Concentration of $[\text{Gd}_2\text{-3}] = 2.38 \text{ mM}$.

the value reported for other related complexes.^[1b] The correlation time modulating the electronic relaxation (τ_v) and the electronic relaxation time at zero field ($\tau_{SO} = (12\Delta^2\tau_v)^{-1}$) were optimized for the outer-sphere and inner-sphere contributions, simultaneously. The distance (r) between the protons of the coordinated water molecule and the Gd^{3+} ion was set to 0.31 nm. At 20 MHz and 37 °C the relaxivity of $[Gd_2-3]$, expressed in 6.8 s^{-1} per mmol of Gd^{3+} , is higher than that of $[Gd(DTPA)]$ and $[MS-325]$ (3.9 and $5.5 \text{ s}^{-1} \text{ mmol}^{-1}$, respectively). Moreover, if the relaxivity of $[Gd_2-3]$ is expressed in s^{-1} per mmol of the complex, its value is equal to 13.6 at 37 °C and 0.47 T.

Inspection of the parameters shown in Table 2 reveals that the higher relaxivity of $[Gd_2-3]$ can be related to its larger rotational correlation time (τ_R), that is, to its reduced

Table 2. Parameters obtained from fitting of the proton NMRD data, obtained in water at 310 K, for $[Gd_2-3]$ compared to the data for $[Gd(DTPA)]$ and $[MS-325]$.

Compound	τ_M^{310} [ns]	τ_R^{310} [ps]	τ_{SO}^{310} [ps]	τ_V^{310} [ps]
$[Gd_2-3]$	599	188	82	34
$[Gd(DTPA)]$ ^[a]	143	59	82	23
$[MS-325]$ ^[b]	83	108	93	32

[a] From ref. [25a] [b] From ref. [25c] with a distance $r = 0.31$ nm.

motion. The rate of molecular tumbling observed for $[Gd_2-3]$ is a third of that of the parent $[Gd(DTPA)]$ complex, demonstrating the significant effect of increasing the molecular size of the dinuclear complex. The other parameters (τ_{SO} and τ_v) are in good agreement with those reported for both $[Gd(DTPA)]$,^[31a,b] and $[MS-325]$.^[25a]

Binding of $[Gd_2-3]$ to serum albumin: Contrast agents can interact by noncovalently binding to proteins present in blood plasma. The most important protein in human plasma is serum albumin (HSA), which constitutes 4 to 4.5% of plasma (0.67 mM). This large (67 kDa) globular protein binds to a variety of molecules, such as drugs, metabolites, and fatty acids.^[35] Noncovalent interactions of MRI contrast agents with HSA result in the reduction of the molecular tumbling rate of the contrast agent (i.e., the value of τ_R increases), and hence in an increase in its relaxivity. Figure 4 displays the longitudinal proton relaxation rate in a solution containing 4% HSA, as a function of $[Gd_2-3]$ concentration. The relaxivity of $[Gd_2-3]$ is much greater in a solution of HSA than in pure water, indicating a noncovalent interaction. Binding to albumin reduces the amount of free drug that can extravasate from the blood pool into the nonvascular space and provides the selective enhancement of the vascular relaxation rate. Binding also reduces the fraction of free chelate available for glomerular filtration by the kidneys. This slows the renal excretion rate, which extends the half-life in the blood and increases the time available for imaging.

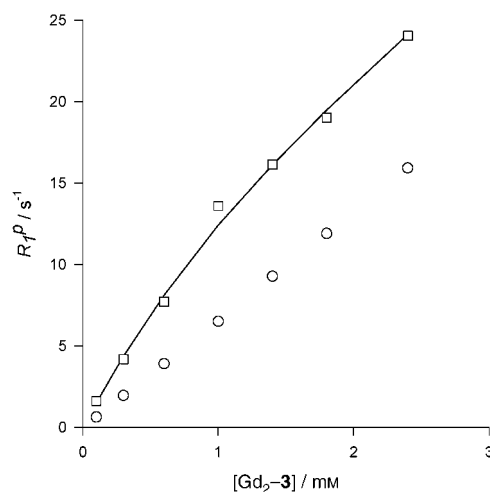


Figure 4. Proton longitudinal paramagnetic relaxation rate in a solution containing 4% HSA and increasing amounts of $[Gd_2-3]$ (\square), at 20 MHz and 310 K. The relaxation rates in the absence of HSA are represented by \circ . The diamagnetic contribution of the albumin solutions was measured by using the solution of 4% HSA.

Fitting of the data by means of Equation (1) provides, on the one hand, an estimation of the association constant K_a , which characterizes the interaction between HSA and $[Gd_2-3]$, and on the other hand, a value for the relaxivity of the noncovalently bound complex, r_1^c . The relaxivity of the free contrast agent, r_1^f , was determined for the dimeric $[Gd_2-3]$ to be 13.6 s^{-1} per mmol of $[Gd_2-3]$ (or 6.8 s^{-1} per mmol of Gd^{3+}), which is larger than the r_1^f value for $[MS-325]$ ($5.5 \text{ s}^{-1} \text{ mmol}^{-1}$) at the same field ($B_0 = 0.4$ T) and temperature ($T = 310$ K).^[25a]

$$R_1^{\text{obs}} = 1000 \times \left\{ (r_1^f \times s^0) + 0.5(r_1^c - r_1^f) \left((N \times p^0) + s^0 + K_a^{-1} - \sqrt{((N \times p^0) + s^0 + K_a^{-1})^2 - 4 \times N \times s^0 \times p^0} \right) \right\} \quad (1)$$

in which p^0 and s^0 are the initial concentrations of protein and $[Gd_2-3]$, respectively.

To fit the data, the number of equivalent and independent interactions sites (N) was set to 1. The fitted K_a and r_1^c values are 10100 M^{-1} and 15.2 s^{-1} per mmol of Gd^{3+} (30.4 s^{-1} per mmol of $[Gd_2-3]$), respectively, which implies that the relaxivity is much higher than the values for the free $[Gd_2-3]$.

This value of r_1^c is lower than those reported for other Gd-complexes, such as $[MS-325]$ ($r_1^c \approx 49 \text{ s}^{-1} \text{ mmol}^{-1}$ in water at 310 K,^[25a] $r_1^c \approx 42\text{--}43 \text{ s}^{-1} \text{ mmol}^{-1}$ at pH 7.5 in Hepes buffer at 310 K,^[25c] or $[Gd-DTPA(BOM)_3]$ (BOM = benzyloxymethyl) ($r_1^c \approx 52 \text{ s}^{-1} \text{ mmol}^{-1}$ at pH 7.5 in Hepes buffer at 310 K^[25c]). This difference can be related to a quenching of the relaxivity of the bound $[Gd_2-3]$ by the long water residence time. In addition, for both $[MS-325]$ and $[Gd-DTPA(BOM)_3]$, only one Gd^{3+} ion is located within the complex, whereas in $[Gd_2-3]$, the two paramagnetic centers are locat-

ed quite far from the area of the complex likely to interact with the protein. Consequently, either both paramagnetic centers will experience the same slowing of their rotational motion, or, if one center is protein-bound, this will experience a larger effect than the other center. However, because both paramagnetic centers of $[\text{Gd}_2\text{-3}]$ could have different rotational mobilities, the relaxometric measurement cannot distinguish between the gadolinium centers. The value calculated by the fitting procedure is, therefore, an average of two different r_1^p values.

Transmetalation of $[\text{Gd}_2\text{-3}]$ by zinc(II): In general, there is no direct correlation between the thermodynamic stability constant and the acute toxicity of contrast agents. The conditional stability constants at physiological pH (7.4) are better indicators of the in vivo degree of chelation of the cation. Cacheris et al. have argued that, due to possible transmetalation reactions in the body, the in vivo toxicity for DTPA derivatives is determined by the selectivity or difference in stability between a complex of ligand with Gd^{3+} , and a complex of that same ligand with Zn^{2+} , thermodynamically expressed as K_{sel} . These authors have shown that $\log K_{\text{sel}}$ at physiological pH correlates with toxicity.^[36] Transmetalation of the complex by Zn^{2+} results in the release of Gd^{3+} ions, which form an insoluble phosphate complex in the presence of phosphate ions, and no longer contribute to the proton paramagnetic relaxation rate of the solution. The consequent decrease in this rate during the transmetalation process can be used to monitor quantitatively the evolution of the system.^[37] Figure 5 displays the transmetalation data for $[\text{Gd}_2\text{-3}]$. After 5000 min, R_1^p is decreased to 40% of its initial value, showing that significant transmetalation takes place. These data are less favorable than those for $[\text{MS-325}]$, in which the R_1^p decreased to about 75% of its initial value after 5000 min.^[25a] However, the data are comparable with those of the parent $[\text{Gd}(\text{DTPA})]$ complex (decrease to

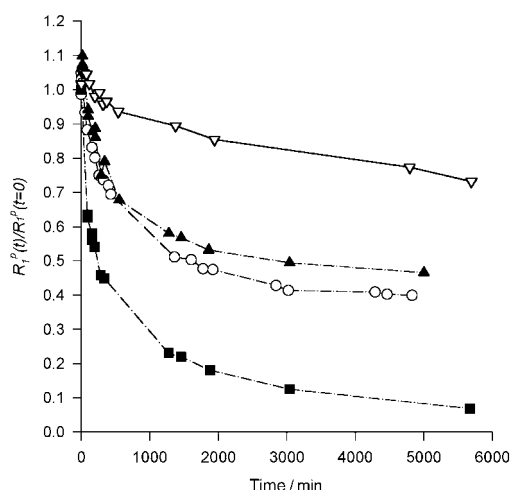


Figure 5. Time course of the normalized water proton paramagnetic relaxation rate at 310 K and 20 MHz in a solution containing 2.5 mM of Zn^{2+} and 2.5 mM of $[\text{Gd}_2\text{-3}]$ (○), $[\text{Gd}(\text{DTPA-BMA})]$ (■), $[\text{Gd}(\text{DTPA})]$ (▲), or $[\text{MS-325}]$ (▽).

49% after 5000 min), and much more favorable than another commercially available $[\text{Gd}(\text{DTPA-BMA})]$ contrast agent, for which the R_1^p decreased to 9% after 5000 min. This indicates that $[\text{Gd}_2\text{-3}]$ has a stability comparable to $[\text{Gd}(\text{DTPA})]$, but appears to be much more stable than the $[\text{Gd}(\text{DTPA-BMA})]$ contrast agent towards transmetalation by zinc(II).

Pharmacokinetic profile of $[\text{Gd}_2\text{-3}]$: The pharmacokinetic profile provides information about both the residence time of $[\text{Gd}_2\text{-3}]$ in the bloodstream, and its clearance after intravenous injection. The profiles of $[\text{Gd}_2\text{-3}]$ in rats with respect to $[\text{Gd}(\text{DTPA})]$ are presented in Figure 6. Pharmacokinetic

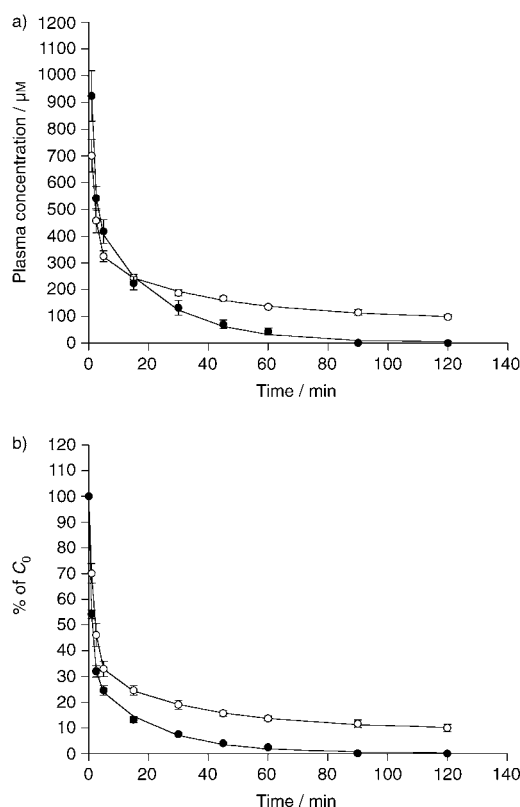


Figure 6. Pharmacokinetic profiles of $[\text{Gd}_2\text{-3}]$ (○, $n=4$) with respect to $[\text{Gd}(\text{DTPA})]$ (●, $n=3$) in rats. Data are presented as absolute values of plasma concentration (top) and percentages of C_0 (bottom). The solid lines represent the fit of the data to a biexponential model. Data points are presented as averages \pm SEM.

parameters were calculated by fitting the curves of blood concentration as a function of time following a single bolus in vivo injection, and are presented in Table 3. Except for the volume of distribution (VD_β), which is comparable to that of $[\text{Gd}(\text{DTPA})]$, the other parameters for $[\text{Gd}_2\text{-3}]$ indicate a significantly prolonged vascular residence time. The delayed blood clearance is probably attributable to the binding of $[\text{Gd}_2\text{-3}]$ to albumin in the blood. Notably, although the VD_β for $[\text{Gd}_2\text{-3}]$ in rats (0.189 L kg^{-1}) is similar to the value for $[\text{Gd}(\text{DTPA})]$, it is even smaller than that of other

albumin-binding blood-pool contrast agents, such as [MS-325] ($VD_{\beta} = 0.236 \text{ L kg}^{-1}$).^[23] The longer elimination half-life indicates that the agent has a long vascular residence, and could have potential as a blood-pool contrast agent.

Table 3. Pharmacokinetic parameters of [Gd₂-3] and [Gd(DTPA)] in rats. $T_{d1/2}$ and $T_{e1/2}$ are the distribution and elimination half-lives in plasma, respectively; Cl_{tot} is the total clearance; VD_{β} is the distribution volume in the elimination phase.

Parameter	[Gd ₂ -3] (n=4)	[Gd(DTPA)] (n=3)
$T_{d1/2}$ [min]	$1.56 \pm 0.025^{[b]}$	0.70 ± 0.039
$T_{e1/2}$ [min]	$75.93 \pm 12.80^{[a]}$	14.94 ± 1.25
Cl_{tot} [$\text{mL kg}^{-1} \text{ min}^{-1}$]	$1.10 \pm 0.15^{[b]}$	8.66 ± 1.18
VD_{β} [L kg^{-1}]	0.189 ± 0.016	0.180 ± 0.005

[a] $p < 0.05$. [b] $p < 0.01$.

Biodistribution of [Gd₂-3]: The biodistribution studies show whether the contrast agent accumulates in specific organs. In good agreement with its slower elimination, the biodistribution of [Gd₂-3] in rats 60 min after intravenous administration (Figure 7) indicates significantly higher concentra-

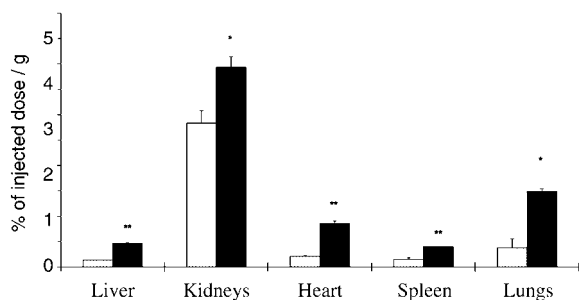


Figure 7. Biodistribution of [Gd₂-3] (black bars) and [Gd(DTPA)] (gray bars) 60 min after administration. The results are presented as averages \pm SEM; the Student t-test was calculated for [Gd₂-3] versus [Gd(DTPA)] (*: $p < 0.05$; **: $p < 0.01$).

tions than [Gd(DTPA)] in all of the organs analyzed. The Gd^{3+} concentration measured in kidney suggests that [Gd₂-3] has a renal route of excretion. On the other hand, the relatively high Gd^{3+} concentration detected in liver (ca. 3.5 times higher than for [Gd(DTPA)]), $p < 0.01$ could be related to its lipophilic properties, leading to a possible hepatobiliary route of excretion. In fact, many albumin-binding complexes are believed to interact with hepatocytes, and although the mechanism of interaction is not completely understood, the dissociated chelate is removed from circulation by the hepatobiliary route.

In vivo evaluation of contrast-enhancing properties and necrosis avidity of [Gd₂-3]: The liver contrast-enhancing efficacy on T_1 -weighted MRI in vivo was evaluated by comparing [Gd₂-3] at an intravenous dosage of $0.05 \text{ mmol kg}^{-1}$ with [Gd(DTPA)] at a dose of 0.1 mmol kg^{-1} in normal rats ($n =$

6). At only half of the dose of [Gd(DTPA)], [Gd₂-3] caused a signal intensity (SI) of the normal liver that was significantly higher over the first 60 min than that measured with [Gd(DTPA)]. Although the liver SI for [Gd(DTPA)] leveled off rapidly within 40 min, in the case of [Gd₂-3], it only slowly decreased over 24 h (Figure 8). Such distinctive con-

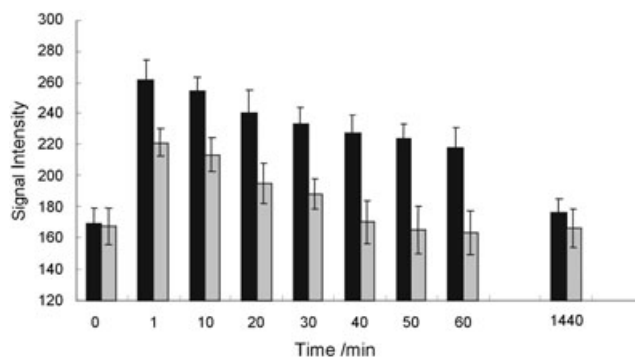


Figure 8. Comparison of the liver signal intensity of T_1 -weighted MR images after intravenous injection of [Gd(DTPA)] at 0.1 mmol kg^{-1} (gray bars) and [Gd₂-3] at $0.05 \text{ mmol kg}^{-1}$ (black bars). Over the first 60 min postcontrast, liver contrast enhancement is significantly stronger with [Gd₂-3] than with the commercially available [Gd(DTPA)].

trasts can be well explained by the different structural properties of [Gd(DTPA)] and [Gd₂-3]; whereas [Gd(DTPA)] is a hydrophilic, extracellular fluid agent, [Gd₂-3] is more lipophilic due to the presence of the trimethoxybenzene ring and two indole moieties, and is, therefore, more likely to be taken up by the liver.

To evaluate whether [Gd₂-3] can act as a potential necrosis avid contrast agent (NACA), we compared it to the well-known NACA Gadophrin-2 in a rat model with re-perfused partial liver infarction. The same dose of [Gd₂-3] and Gadophrin-2 ($0.05 \text{ mmol kg}^{-1}$) caused a prompt contrast enhancement (CE) in normal liver tissue, rendering the infarcted liver lobe easily distinguishable by MRI as a hypointense zone. Contrary to a reversed contrast between infarcted and normal liver lobes that occurred with Gadophrin-2, a continuing liver signal intensity attenuation was observed with [Gd₂-3]. The SI of normal and infarcted liver after [Gd₂-3] injection was normalized overnight with no appreciable necrosis/normal contrast (contrast ratio, $CR \approx 1$). The SI of the infarcted lobe after Gadophrin-2 injection increased further and persisted for up to 24 h, leading to a positive contrast between necrotic and normal liver ($CR = 1.4$), consistent with results of previous studies.^[38,39]

Despite its high albumin-binding affinity, [Gd₂-3] does not appear to be a necrosis avid contrast reagent, supporting the suggestion that binding to albumin is probably not responsible for necrosis avidity. This is not unexpected, as albumin binding is a general feature of many drugs, including contrast agents, only a few of which have been shown to have necrosis avidity.^[40] However, it is notable that with half

of the normal dose, $[Gd_2-3]$ enhances the contrast in liver tissues much more effectively than does $[Gd(DTPA)]$.

Conclusion

A new type of contrast agent bearing two DTPA units able to bind two paramagnetic centers has been synthesized, characterized, preclinically evaluated, and tested for necrosis avidity. Data from NMRD analysis proved that the dimeric complex has a much higher relaxivity than $[Gd(DTPA)]$, and that the relaxivity increases significantly in a solution of human serum albumin because of a relatively strong interaction with this blood protein. The interaction with HSA also results in longer elimination half-lives and a better confinement to the vascular space, as shown by pharmacokinetic evaluation. The fact that two gadolinium(III) ions are present in one molecule of the contrast agent permits the use of smaller injection volumes. With half the normal dose, the dimeric complex enhanced the contrast in tissues more effectively than $[Gd(DTPA)]$.

The synthetic approach described here offers the potential to design high molecular weight contrast agents with defined structure. The increase in relaxivity achieved is due not only to the longer rotational correlation times, but also to the interaction of the linker with HSA. Application of this strategy should facilitate the use of many different types of linkers with high affinities towards blood proteins.

Experimental Section

Materials: Reagents were obtained from Aldrich Chemical (Bornem, Belgium), Acros Organics (Beerse, Belgium), and Fluka (Bornem, Belgium), and used without further purification. Gadolinium(III) chloride hexahydrate was obtained from GFS chemicals (Powell, Ohio, USA). Non-defatted human albumin (fraction V) was obtained from Sigma (Bornem, Belgium).

Syntheses

Preparation of compound 1: Some 3,4,5-trimethoxybenzaldehyde (10.8 g, 55 mmol) was added to a solution of ethylindole-2-carboxylate (18.9 g, 100 mmol) in ethanol (200 mL) under a nitrogen atmosphere, and the mixture was heated to reflux temperature. Concentrated hydrochloric acid (3.7 mL) was added, and TLC on silica gel plates with the chloroform/hexane (1:1) solvent system was used to monitor the reaction by the disappearance of the ethylindole-2-carboxylate ($R_f=0.7$) and the appearance of the reaction product spot ($R_f=0.1$). After about 1 h, the solution was left to cool to room temperature and the white product was filtered off and washed thoroughly with cold ethanol. Yield: 24 g (88%); 1H NMR (300 MHz, $[D_6]DMSO$): $\delta=1.19$ (t, 6H; $2\times CH_3$), 3.46 (s, 6H; $2\times CH_3$), 3.66 (s, 3H; $1\times CH_3$), 4.23 (q, 4H; $2\times CH_2$), 6.43 (s, 2H; Ph), 6.55 (m, 2H; Ph), 6.69 (m, 2H; $2\times Ph$), 6.86 (s, 1H; CH-Ph), 7.12 (m, 2H; Ph), 7.46 (m, 2H; Ph), 11.69 ppm (s, 2H; $2\times NH$); ES-MS (positive mode): m/z : 557.2 $[M+H]^+$.

Preparation of compound 2: Hydrazine monohydrate (50 mL) in methanol (50 mL) was added to a solution of product 1 (16.2 g, 30 mmol) in pyridine (150 mL), and the mixture was heated at 100°C for 36 h. The reaction was monitored by conducting reversed phase HPLC; a peak was detected at 7.3 min (Hypersil BDS 5 μ m column 4.6 mm \times 250 mm (Alltech, Laarne, Belgium), detection wavelength 254 nm, linear gradient from 5 to 95% CH_3CN over 20 min, mobile phase 0.05 M $NaHCO_3$ adjust-

ed to pH 7 with 0.1 M HCl, containing 0.5 mM EDTA; flow rate 1 mL min $^{-1}$). After removal of the solvent, the residue was dissolved in 200 mL of water and the solution was evaporated again. This process was repeated until no free hydrazine could be detected in the solution by using I_2 . The product was then suspended in acetonitrile and filtered. Yield: 14.1 g (90%); 1H NMR (300 MHz, $[D_3]CD_3OH$): $\delta=3.45$ (s, 6H; $2\times CH_3$), 3.66 (s, 3H; $1\times CH_3$), 6.43 (s, 2H; Ph), 6.55 (d, 2H; Ph), 6.69 (m, 2H; Ph), 6.86 (s, 1H; CH-Ph), 7.28 (m, 2H; Ph), 7.45 (m, 2H; Ph), 11.70 ppm (s, 2H; $2\times NH$); ES-MS (positive mode): m/z : 529.2 $[M+H]^+$.

Preparation of compound 3: A dispersion of DTPA (61 g, 155 mmol) in a mixture of DMSO (1800 mL) and triethylamine (TEA, 50 mL; 36 g, 0.36 mol) was sonicated for 15 min. TBTU (25 g, 78 mmol) was added and the mixture was sonicated again for 15 min. Product 2 (10.44 g, 20 mmol) was added and the mixture was stirred for 1 h. After removal of the solvent, the residue was dissolved in a concentrated solution of $NaHCO_3$. The pH was adjusted to 7 with concentrated hydrochloric acid, followed by sonication for 30 min. The resulting mixture was evaporated and placed on a C_{18} reversed-phase column (10 mm \times 80 cm), which was then eluted successively with 5 L of a solution of ammonium acetate in distilled water (0.1 M) containing 2.5% methanol, 3 L of a solution containing 5% methanol, and finally with 3 L of a solution containing 10% methanol. The product was collected in 200 mL fractions and the purity was checked by conducting HPLC (conditions as for the preparation of 2, above) and monitoring the peak eluting at 4.4 min. Yield: 13 g (51%); 1H NMR (300 MHz, D_2O , pD=6.0): $\delta=3.11$ (m, 8H; $2\times N-CH_2$), 3.27 (m, 4H; $2\times N-CH_2$), 3.37 (m, 4H; $2\times N-CH_2$), 3.43 (s, 4H; $2\times CH_2-COOH$), 3.53 (s, 8H; $4\times CH_2-COOH$), 3.65 (s, 9H; $3\times OCH_3$), 3.69 (b, 8H; $2\times CH_2-COOH$, $2\times CH_2-CO-NH$), 6.66 (s, 2H; Ph), 6.75 (m, 2H; Ph), 6.79 (m, 2H; Ph), 6.86 (s, 1H; CH-Ph), 7.19 (m, 2H; Ph), 7.45 ppm (m, 2H; Ph); IR (KBr): $\tilde{\nu}=3406$ (N-H), 3008 (C-H, phenyl), 2917 and 2852 (C-H alkyl), 1687 (CO, amide I), 1624 (CO acid), 1591 (COO $^-$ assym. stretch), 1404 cm^{-1} (COO $^-$ sym. stretch); elemental analysis calcd (%) for $NaC_{56}N_{12}O_{23}H_{65}(NH_4)_4$: C 48.66, H 6.39, N 16.33; found: C 49.1, H 6.0, N 16.36; ES-MS (positive mode): m/z : 1301.4 $[M+Na]^+$, 662.3 $[M+2Na]^+$.

Synthesis of the lanthanide(III) complexes

The lanthanide(III) complexes of ligand 3 were synthesized according to a general procedure as follows: a solution of hydrated $LnCl_3$ salt (1.1 mmol) in H_2O (1 mL) was added to ligand 3 (0.5 mmol) dissolved in pyridine (30 mL), and the mixture was heated at 70°C for 3 h. The solvents were evaporated under reduced pressure and the crude product was then refluxed in ethanol for 1 h. After cooling to room temperature, the complex was filtered off and dried in a vacuum. The absence of free gadolinium was verified by using xylenol orange indicator.^[41]

Lanthanum(III) complex $[La_2-3]$: Yield: 95% (1.51 g); IR (KBr): $\tilde{\nu}=3401$ (N-H), 3016 (C-H, phenyl), 2922 and 2850 (C-H alkyl), 1630 (CO, amide I), 1590 (COO $^-$ assym. stretch), 1400 cm^{-1} (COO $^-$ sym. stretch); elemental analysis calcd (%) for $La_2C_{56}N_{12}O_{23}H_{62}Na_2(H_2O)_4$: C 40.51, H 4.75, N 10.04; found: C 40.30, H 4.23, N 10.08; ES-MS (positive mode): m/z : 1595 $[M+H]^+$, 1613 $[M+H+H_2O]^+$, 1635 $[M+Na+H_2O]^+$, 798 $[M+2H]^+$.

Gadolinium(III) complex $[Gd_2-3]$: Yield: 96% (1.56 g); IR (KBr) $\tilde{\nu}=3406$ (N-H), 2915 and 2840 (C-H alkyl), 1637 (CO amide I), 1585 (COO $^-$ assym. stretch), 1404 cm^{-1} (COO $^-$ sym. stretch); elemental analysis calcd (%) for $Gd_2C_{56}N_{12}O_{23}H_{62}Na_2(H_2O)_8$: C 37.65, H 4.91, N 9.90; found: C 37.87, H 4.43, N 9.47; ES-MS (positive mode): m/z : 1632 $[M+H]^+$, 1610 $[M-Na+2H]^+$, 795 $[M-2Na+4H]^+$.

Instruments: Elemental analysis was performed by using a CE Instruments EA-1110 elemental analyzer. 1H NMR spectra were recorded by using a Bruker Avance 300 (Bruker, Karlsruhe, Germany), operating at 300 MHz. IR spectra were measured by using an FTIR spectrometer Bruker IFS66, using the KBr pellet method. Mass spectra were obtained by using a Q-tof 2 (Micromass, Manchester, UK). Samples for the mass spectrometry were prepared by dissolving the complex (2 mg) in methanol (1 mL), then adding 200 μ L of this solution to a water/methanol mixture (50:50, 800 μ L). The resulting solution was injected at a flow rate of 5 μ L min $^{-1}$.

^{17}O NMR measurements: Samples of solutions (2 mL) contained in NMR tubes (OD 10 mm) were analyzed by using an AMX-300 spectrometer (Bruker, Karlsruhe, Germany). The temperature was regulated by air or nitrogen flow controlled by a BVT 2000 unit (Bruker, Karlsruhe, Germany). No field frequency lock was used. All ^{17}O NMR spectra were proton decoupled. The ^{17}O transverse relaxation times of distilled water were measured by using a CPMG (Car–Purcell Meiboom Gill) sequence and a subsequent two-parameters-fit of the data points. The 90 and 180° pulse lengths were 25 and 50 μs , respectively. The ^{17}O T_2 of the complex in aqueous solution was obtained from line width measurement. The concentration of the samples was less than 25 mM.

T_1 measurements: Proton nuclear magnetic relaxation dispersion (NMRD) profiles were recorded between 0.24 mT and 0.24 T by using Field Cycling Relaxometers (Field Cycling Systems, Oradell, New Jersey, USA and Stelar Spinmaster FFC-2000, Stelar SRL, Mede, Italy) with 0.6 mL solutions contained in 10 mm OD tubes. Proton relaxation rates were also measured at 0.47 T and 1.4 T by using Minispec PC-120 and mq-60, respectively (Bruker, Karlsruhe, Germany). The temperature was maintained at 310 K. ^1H NMRD data were fitted according to the theoretical inner-sphere model described by Solomon^[32] and Bloembergen,^[33] and to the outer-sphere contribution described by Freed.^[34] Calculations were performed by using a previously described software package.^[42–43]

Transmetalation: Transmetalation by zinc(II) ions was evaluated by the decrease in the water longitudinal relaxation rate at 310 K and 20 MHz (Bruker Minispec PC-120) of buffered phosphate solutions (pH 7, $[\text{KH}_2\text{PO}_4]=26$ mM, $[\text{Na}_2\text{HPO}_4]=41$ mM) containing 2.5 mM of the gadolinium(III) complex and 2.5 mM of Zn^{2+} .^[37]

Interaction with HSA: The binding constant and relaxivity value of $[\text{Gd}_2\text{—}3]$ in a 4% solution of HSA was determined by measuring the proton longitudinal relaxation rate at 20 MHz and 310 K as a function of the $[\text{Gd}_2\text{—}3]$ concentration.

In vivo characterization: All of the animal experiments were performed according to recommendations of the ethical commission of K.U.Leuven and the University of Mons-Hainaut.

Pharmacokinetic characterization: The animals were anesthetized by the intraperitoneal injection of pentobarbital (Nembotal[®], Sanofi Sante Animale, Brussels, Belgium) at a dose of 60 mg kg^{-1} . Wistar rats ($n=3$ or 4/group, 269 $\text{g} \pm 6$ g, Harlan, The Netherlands) were tracheotomized and the left carotide was catheterized (Becton Dickinson Angiocath, 0.7 \times 19 mm) for blood collection. The agent was administered as a bolus in the femoral vein at a dose of 0.025 mmol kg^{-1} (0.05 mmol of gadolinium per kg). $[\text{Gd}(\text{DTPA})]$, used as a control, was injected at a dose of 0.1 mmol kg^{-1} . Blood samples (~0.3 mL) were collected 1, 2.5, 5, 15, 30, 45, 60, 90, and 120 min after injection. The concentration of gadolinium in the blood samples was determined by conducting relaxometry at 37°C and 60 MHz with a Bruker Minispec mq60 (Bruker, Karlsruhe, Germany).^[45] A two-compartment distribution model was used to calculate the distribution ($T_{d1/2}$) and elimination ($T_{e1/2}$) half-lives, the apparent volume of distribution (VD_p), the total clearance (Cl_{tot}), and the initial blood concentration C_0 .^[23] The gadolinium concentrations in blood were converted to plasma concentrations by assuming a hematocrit value of 0.53.^[44]

Biodistribution: Adult Wistar rats ($n=3/\text{group}$, 273 $\text{g} \pm 9$ g, Harlan, The Netherlands) were anesthetized and injected with the contrast agents, as described above. Sixty minutes after injection, the animals were sacrificed and samples of liver, kidneys, heart, lungs, and spleen were collected for evaluation of the gadolinium content. The samples were weighed, dried overnight at 60°C, and subsequently digested (up to 0.4 g each sample) in acidic conditions (3 mL HNO_3 65%, 1 mL H_2O_2 33%) by microwaves (Milestone MSL-1200, Sorisole, Italy). The gadolinium content was determined by performing inductively coupled plasma atomic emission spectroscopy (ICP-AES, Jobin Yvon JY70+, Longjumeau, France). The gadolinium concentration was expressed as a percentage of the injected dose per gram of tissue.

In vivo evaluation for liver contrast enhancement: Six normal rats and a rat with re-perfused hepatic infarction induced under laparotomy with temporary obstruction (3 h) of the blood supply to the right liver lobes^[38,39] were included in MRI studies. Two reference contrast agents were

commercially available; $[\text{Gd}(\text{DTPA})]$, and the well-known NACA bis-Gd-mesoporphyrin or Gadophrin-2 (supplied by the Institut für Diagnostikforschung Berlin, Germany).^[47]

MR imaging and quantification: The rat under anesthesia was placed supinely into a plastic holder. A tail vein of the rat was cannulated with a G27 infusion set connected to a 1 mL tuberculin syringe loaded with a contrast agent. MR imaging was performed using a 1.5 T Siemens Sonata scanner (Erlangen, Germany) with a commercially available four-channel phased-array wrist coil. A T_1 -weighted ($\text{TR}/\text{TE}=600$ ms/15 ms) spin-echo 2D-imaging sequence, with 2 mm slice thickness (without gap), a field of view of 4.6 $\text{cm} \times 8.0$ cm, a 240 \times 512 matrix, and four averaged acquisitions, resulting in about 3 min of measurement, was recorded to study the contrast agents for in vivo contrast enhancement. The SI was measured for a region of interest on five consecutive liver slices on MR images and averaged for precontrast and serial postcontrast phases. The conspicuity of the necrotic lobe was expressed as the contrast ratio (CR) between the necrotic and the normal liver, and was calculated as $\text{CR}=\text{SI}_{\text{necrosis}}/\text{SI}_{\text{normal}}$.

Acknowledgements

T.N.P.V. and K.B. acknowledge F.W.O. Flanders (Belgium) for a Postdoctoral Fellowship. T.N.P.V., K.K., and K.B. also thank the K.U. Leuven for financial support (VIS/01/006.01/20002–06/2004 and GOA 03/03). CHN microanalyses were performed by Mrs. Petra Bloemen. ES-MS measurements were made by Ms. Leen Vannerum. Mrs Corinne Piérart and Mrs Virginie Henrotte are acknowledged for their help in measuring the proton relaxation rates. S.L., L.V.E., C.B., and R.N.M. thank the ARC Program 00/05–258 of the French Community of Belgium and kindly acknowledge the support and sponsorship provided by COST Action D18 “Lanthanide Chemistry for Diagnosis and Therapy”.

- [1] a) R. B. Lauffer, *Chem. Rev.* **1987**, *87*, 901–927; b) P. Caravan, J. J. Ellison, T. J. McMurry, R. B. Lauffer, *Chem. Rev.* **1999**, *99*, 2293–2352.
- [2] S. Aime, M. Botta, M. Fasano, E. Terreno, *Chem. Soc. Rev.* **1998**, *27*, 19–29.
- [3] H. J. Weinmann, W. Ebert, B. Misslewitz, H. Schmitt-Willich, *Eur. J. Radiol.* **2003**, *46*, 33–44.
- [4] D. J. Hnatowich, B. Friedman, B. Clancy, M. Novak, *J. Nucl. Med.* **1981**, *22*, 810–814.
- [5] G. W. Kabalka, M. A. Davis, T. H. Moss, E. Buonocore, K. Hubner, E. Holmberg, K. Maruyama, L. Huang, *Magn. Reson. Med.* **1991**, *19*, 406–415.
- [6] E. C. Unger, D. K. Shen, T. A. Fritz, *J. Magn. Reson. Imaging* **1993**, *3*, 195–198.
- [7] É. Tóth, D. Pubanz, S. Vauthey, L. Helm, A. E. Merbach, *Chem. Eur. J.* **1996**, *2*, 1607–1615.
- [8] M. Spanoghe, D. Lanens, R. Dommissie, A. van der Linden, F. Alderweireldt, *Magn. Reson. Imaging* **1992**, *10*, 913–917.
- [9] V. S. Vexler, O. Clement, H. Schmitt-Willich, R. C. Brasch, *J. Magn. Reson. Imaging* **1994**, *4*, 381–388.
- [10] T. S. Desser, D. L. Rubin, H. H. Muller, F. Qing, S. Khodor, G. Zanzani, S. U. Young, D. L. Ladd, J. A. Wellons, K. E. Kellar, J. L. Toner, R. A. Snow, *J. Magn. Reson. Imaging* **1994**, *4*, 467–472.
- [11] S. Aime, M. Botta, M. Fasano, S. G. Crich, E. Terreno, *J. Biol. Inorg. Chem.* **1996**, *1*, 312–319.
- [12] É. Tóth, F. Connac, L. Helm, K. Adzamlı, A. E. Merbach, *J. Biol. Inorg. Chem.* **1998**, *3*, 606–613.
- [13] S. W. A. Bligh, A. H. M. S. Chowdhury, M. McPartlin, I. J. Scowen, R. A. Bulman, *Polyhedron* **1995**, *14*, 567–569.
- [14] S. Aime, M. Botta, M. Fasano, E. Terreno, *Chem. Soc. Rev.* **1998**, *27*, 19–29.
- [15] K. Kimpe, T. N. Parac-Vogt, S. Laurent, C. Piérart, L. Vander Elst, R. N. Muller, K. Binnemans, *Eur. J. Inorg. Chem.* **2003**, 3021–3027.

- [16] P. L. Anelli, L. Lattuada, V. Lorusso, M. Schneider, H. Tournier, F. Uggeri, *MAGMA* **2001**, *12*, 114–120.
- [17] J. P. André, É. Tóth, H. Fischer, A. Seelig, H. R. Mäcke, A. E. Merbach, *Chem. Eur. J.* **1999**, *5*, 2977–2983.
- [18] K. Binnemans, C. Görrler-Walrand, *Chem. Rev.* **2002**, *102*, 2303–2345.
- [19] H. Tournier, B. Lamy, R. Hyacinthe, US-5.833.948, **1998**.
- [20] B. G. Jenkins, E. Armstrong, R. B. Lauffer, *Magn. Reson. Med.* **1991**, *17*, 164–178.
- [21] R. B. Lauffer, *Magn. Reson. Med.* **1991**, *22*, 339–342.
- [22] R. B. Lauffer, D. J. Parmelee, H. S. Ouellet, R. P. Dolan, H. Sajiki, D. M. Scott, P. J. Bernard, E. M. Buchanan, K. Y. Ong, Z. Tyeklar, K. S. Midelfort, T. J. McMurry, R. C. Walovitch, *Acta Radiol.* **1996**, *3*, S356–S358.
- [23] D. J. Parmelee, R. C. Walovitch, H. S. Ouellet, R. B. Lauffer, *Invest. Radiol.* **1997**, *32*, 741–747.
- [24] R. B. Lauffer, D. J. Parmelee, S. U. Dunham, H. S. Ouellet, R. P. Dolan, S. Witte, T. J. McMurry, R. C. Walovitch, *Radiology* **1998**, *207*, 529–538.
- [25] a) R. N. Muller, B. Raduchel, S. Laurent, J. Platzek, C. Piérart, P. Mareski, L. Vander Elst, *Eur. J. Inorg. Chem.* **1999**, 1949–1955; b) P. Caravan, N. J. Cloutier, M. T. Greenfield, S. A. McDermid, S. U. Dunham, J. W. M. Bulte, J. C. Amedio, R. J. Looby, R. M. Supowski, W. D. Horrocks, T. J. McMurry, R. B. Lauffer, *J. Am. Chem. Soc.* **2002**, *124*, 3152–3162; c) S. Aime, M. Chiaussa, G. Digilio, E. Gianolio, E. Terreno, *J. Biol. Inorg. Chem.* **1999**, *4*, 766–774.
- [26] B. Hofmann, A. Bogdanov, E. Marecos, W. Ebert, W. Semmler, R. Weissleder, *J. Magn. Reson. Imaging* **1999**, *9*, 336–341.
- [27] a) J. F. Desreux, J. Vincent, V. Humblet, M. Hermann, V. Comblin-Tholet, M. F. Tweedle, US-6.056.939, **2000**; b) R. Ruloff, G. van Kotten, A. E. Merbach, *Chem. Commun.* **2004**, 842–843.
- [28] V. V. Martin, W. H. Ralston, M. R. Hynes, J. F. W. Keana, *Bioconjugate Chem.* **1995**, *6*, 616–623.
- [29] E. P. Mayoral, M. García-Amo, P. López, E. Soriano, S. Cerdán, P. Ballesteros, *Bioorg. Med. Chem.* **2003**, *11*, 5555–5567.
- [30] C. F. G. C. Geraldés, A. M. Urbano, M. A. Hoefnagel, J. A. Peters, *Inorg. Chem.* **1993**, *32*, 2426–2432.
- [31] a) S. Laurent, L. Vander Elst, S. Houzé, N. Guérit, R. N. Muller, *Helv. Chim. Acta* **2000**, *83*, 394–406; b) D. H. Powell, O. M. NiDhubhghaill, D. Pubanz, L. Helm, Y. S. Lebedev, W. Schlaeffer, A. Merbach, *J. Am. Chem. Soc.* **1996**, *118*, 9333–9346.
- [32] I. Solomon, *Phys. Rev.* **1955**, *99*, 559–565.
- [33] N. Bloembergen, *J. Chem. Phys.* **1957**, *27*, 572–573.
- [34] J. H. Freed, *J. Chem. Phys.* **1978**, *68*, 4034–4037.
- [35] T. J. Peeters, *All about Albumin: Biochemistry, Genetics and Medical Applications*, Academic Press, San Diego, **1996**.
- [36] W. P. Cacheris, S. C. Quay, S. M. Rocklage, *Magn. Reson. Imaging* **1990**, *8*, 467–481.
- [37] S. Laurent, L. Vander Elst, F. Copoix, R. N. Muller, *Invest. Radiol.* **2001**, *36*, 115–122.
- [38] Y. C. Ni, K. Adzamli, Y. Miao, E. Cresens, J. Yu, M.-P. Periasamy, M. D. Adams, G. Marchal, *Invest. Radiol.* **2001**, *36*, 97–103.
- [39] Y. Ni, C. Petré, Y. Miao, J. Yu, E. Cresens, P. Adriaens, H. Bosmans, W. Semmler, A. L. Baert, G. Marchal, *Invest. Radiol.* **1997**, *32*, 770–779.
- [40] Y. Ni, E. Cresens, P. Adriaens, Y. Miao, K. Verbeke, S. Dymarkoski, A. Verbruggen, G. Marchal, *Acta Radiol.* **2002**, *9*, S98–S101.
- [41] G. Brunisholz, M. Randin, *Helv. Chim. Acta* **1959**, *42*, 1927.
- [42] R. N. Muller, D. Declercq, P. Vallet, F. Giberto, B. Daminet, H. W. Fischer, F. Maton, Y. Van Haverbeke, in *Proceedings, ESMRMB, 7th Annual Congress*, Strasbourg (France), **1990**, 394.
- [43] P. Vallet, Ph.D. thesis, University of Mons-Hainaut (Belgium), **1992**.
- [44] B. Misselwitz, H. Schmitt-Willich, W. Ebert, T. Frenzel, H. J. Weinmann, *MAGMA* **2001**, *12*, 128–134.
- [45] C. Burtea, S. Laurent, J. M. Colet, L. Vander Elst, R. N. Muller, *Invest. Radiol.* **2003**, *38*, 320–333.
- [46] R. Knorr, A. Trzeciak, W. Bannwarth, D. Gillessen, *Tetrahedron. Lett.* **1989**, 1927–1930.
- [47] Y. Ni, G. Marchal, J. Yu, G. Lukito, C. Petré, M. Wevers, A. L. Baert, W. Ebert, C. S. Hilger, F. K. Maier, W. Semmler, *Acad. Radiol.* **1995**, *2*, 687–699.

Received: November 25, 2004
Published online: March 17, 2005